

Vibration Induced Non-adiabatic Geometric Phase and Energy Uncertainty of Fermions in Graphene

SHI-JIE XIONG¹ and YE XIONG²

¹ *National Laboratory of Solid State Microstructures and Department of Physics, Nanjing University, Nanjing 210093, China*

² *College of Physical Science and Technology, Nanjing Normal University, Nanjing 210097, China*

PACS 03.65.Vf – Phases: geometric; dynamic or topological

PACS 73.21.-b – Electron states and collective excitations in multilayers, quantum wells, mesoscopic, and nanoscale systems

PACS 81.05.Uw – Carbon, diamond, graphite

Abstract. - We investigate geometric phase of fermion states under relative vibrations of two sublattices in graphene by solving time-dependent Schrödinger equation using Floquet scheme. In a period of vibration the fermions acquire different geometric phases depending on their momenta. There are two regions in the momentum space: the adiabatic region where the geometric phase can be approximated by the Berry phase and the chaotic region where the geometric phase drastically fluctuates in changing parameters. The energy of fermions due to vibrations shows spikes in the chaotic region. The results suggest a possible dephasing mechanism which may cause classical-like transport properties in graphene.

Due to advances of material science, the graphene, as a two-dimensional (2D) system with one layer of carbon atoms, has been fabricated recently. Graphene exhibits striking properties which attracted much attention of both experimentalists and theorists [1–14]. Particularly, the Dirac dispersion relation of electrons in graphene and the Fermi level near the Dirac point lead to specific features different from those in usual metals and semiconductors. There exists a universal maximal resistivity, independent of their shapes and mobility. Moreover, it is found that the weak localization is strongly suppressed [6] that could be attributed to a dephasing effect similar to the phase uncertainty caused by random magnetic field. There are several theoretical studies using different methods addressing the unusual transport properties in graphene [7–14].

The effect of the Berry phase acquired by fermions in cyclic motions around the Dirac point has been noticed both theoretically [15] and experimentally [3]. **The non-adiabatic effects and Kohn anomaly due to electron-phonon interaction have also been addressed recently [16].** In this paper we investigate the geometric phase of fermions induced by periodic vibrations between two sublattices. It is shown that in a period of vibration the geometric phase acquired by fermions can be expressed by the adiabatic theory only in the momentum region where the level splitting of fermions in the evolution path is much larger than $\hbar\omega$ with ω being the frequency. Outside this region the adiabatic condition is not satisfied. We show that the geometric phase, the fermion average energy, and the energy uncertainty in the non-adiabatic region are much different from those in the adiabatic region.

The fermion band in graphene can be described by a tight-binding Hamiltonian with one π orbital per site on a 2D honeycomb lattice [17]:

$$H = \sum_{\langle nn' \rangle} t_{nn'} (a_n^\dagger a_{n'} + a_{n'}^\dagger a_n), \quad (1)$$

where a_n^\dagger (a_n) creates (annihilates) an electron at site n , $\langle \dots \rangle$ denotes the nearest-neighbor (NN) sites, and $t_{nn'}$ is the NN hopping. The spin indices are not explicitly included. On a honeycomb lattice there are two sublattices, labeled as A and B. On a perfect lattice, all the NN hopping integrals are the same, $t_{nn'} = t_0$. When there is a displacement \mathbf{d} between two sublattices, the lengths of three NN bonds connected to a site of sublattice A become $l^{(j)} = \sqrt{[d \sin(\theta - \alpha^{(j)})]^2 + [l_0 - d \cos(\theta - \alpha^{(j)})]^2}$, where $j = 1, 2, 3$ labels the three NN bonds, θ is the angle of \mathbf{d} related to the x axis, l_0 is the original bond length, and $\alpha^{(j)} = 0, \frac{2\pi}{3}, -\frac{2\pi}{3}$ for $j = 1, 2, 3$, respectively, is the original azimuth angle of the j th bond. For a small displacement, we can keep only the first-order terms of d and obtain $l^{(j)} \sim l_0 - d \cos(\theta - \alpha^{(j)})$. The corresponding hopping integrals become $t^{(j)}(\mathbf{d}) = t_0 + \lambda d \cos(\theta - \alpha^{(j)})$, with λ being the coefficient of linear dependence of $t^{(j)}(\mathbf{d})$ on $l^{(j)}$.

By using Bloch transformation for electron operators the original Hamiltonian becomes

$$H_0 = \sum_{\mathbf{k}} t_0 \left[e^{ik_x l_0} + 2e^{-ik_x l_0/2} \cos\left(\frac{\sqrt{3}}{2} k_y l_0\right) \right] a_{\mathbf{k}}^\dagger b_{\mathbf{k}} + \text{H.c.} \quad (2)$$

where $a(b)_{\mathbf{k}}$ is annihilation operator of electron on sublattice A(B) with Bloch wavevector \mathbf{k} . Expanding it to the first order of \mathbf{k} around two irreducible K points $\left(0, \mp \frac{4\pi}{3\sqrt{3}l_0}\right)$ in the Brillouin zone, one has

$$H_0 = \frac{3}{2} \sum_{\mathbf{k}} [t_0 l_0 k_y \hat{\tau}_z \otimes \hat{\sigma}_x - t_0 l_0 k_x \hat{\mathbf{1}} \otimes \hat{\sigma}_y], \quad (3)$$

where $\hat{\mathbf{1}}$ and $\hat{\tau}_z$ are unit and Pauli matrices acting on two valleys at two irreducible K points, and $\hat{\sigma}_{x,y}$ are Pauli matrices on two sublattices. The interaction between electrons and lattice displacement \mathbf{d} is

$$H_1 = \sum_{\langle nn' \rangle} (t_{nn'}(\mathbf{d}) - t_0) (a_n^\dagger a_{n'} + a_{n'}^\dagger a_n), \quad (4)$$

where $t_{nn'}(\mathbf{d})$ is the hopping integral between sites n and n' under displacement \mathbf{d} . Keeping only the terms of the first order of \mathbf{d} , the interaction Hamiltonian becomes

$$H_1 = \frac{3\lambda}{2} \sum_{\mathbf{k}} (d_x \hat{\mathbf{1}} \otimes \hat{\sigma}_x + d_y \hat{\tau}_z \otimes \hat{\sigma}_y). \quad (5)$$

It is similar to the expression previously derived based on a valence-force-field model [18]. We only consider in-plane optical modes at the long wavelength limit, as the modes with short wave lengths induce large momentum transfer which causes the electron states out of the Dirac fermion region, the vertical optical modes only quadratically couple with the fermions, and the coupling between acoustic modes and electrons is even more weak as the nearest-neighbor bond lengths are almost unchanged. We denote the in-plane vibrations of the relative coordinates as $d_x = \frac{\eta_x}{\lambda} \cos(\omega t + \alpha_x)$ and $d_y = \frac{\eta_y}{\lambda} \cos(\omega t + \alpha_y)$, where $\frac{\eta_{x(y)}}{\lambda}$ and $\alpha_{x(y)}$ are amplitude and initial phase of the vibration in the $x(y)$ direction, respectively.

The Hamiltonian for electrons becomes time-dependent:

$$H(t) = \frac{3}{2} \sum_{\mathbf{k}} [(t_0 l_0 k_y \hat{\tau}_z + \eta_x \cos(\omega t + \alpha_x) \hat{\mathbf{1}}) \otimes \hat{\sigma}_x - (t_0 l_0 k_x \hat{\mathbf{1}} - \eta_y \cos(\omega t + \alpha_y) \hat{\tau}_z) \otimes \hat{\sigma}_y]. \quad (6)$$

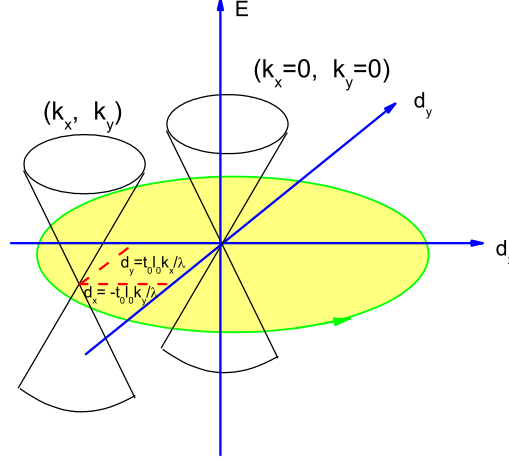


Fig. 1: (Color online) $E_{1,2}^{(+)}$ as functions of \mathbf{d} for different values of \mathbf{k} . Green circle shows the evolution path in the vibrations.

For a given valley labeled by + or -, the Hamiltonian is:

$$H_{\pm}(t) = \frac{3}{2} \sum_{\mathbf{k}} \{t_0 l_0 (\pm k_y \hat{\sigma}_x - k_x \hat{\sigma}_y) + \eta_x \cos(\omega t + \alpha_x) \hat{\sigma}_x \pm \eta_y \cos(\omega t + \alpha_y) \hat{\sigma}_y\}. \quad (7)$$

At the adiabatic limit, the instantaneous eigenenergies at time t can be obtained by diagonalizing $H_{\pm}(t)$:

$$E_m^{(\pm)}(t) = (-1)^m \frac{3}{2} |t_0 l_0 (\pm k_y + i k_x) + \eta_x \cos(\omega t + \alpha_x) \mp i \eta_y \cos(\omega t + \alpha_y)|, \quad (8)$$

where $m = 1$ and $m = 2$ correspond to bands below and above the Dirac point, respectively. For given (k_x, k_y) , these instantaneous eigenenergies exhibit conic dependence on parameters d_x and d_y , as shown in Fig. 1. The diabolical point, where the poles of two cones coincide, is determined by $(d_x = \mp t_0 k_y l_0 / \lambda, d_y = \pm t_0 k_x l_0 / \lambda)$, where plus and minus signs refer to two valleys. The vibrations of d_x and d_y result in circular motion with an elliptic track in the $d_x - d_y$ plane. From the Berry theorem, a cyclic motion along a close track in a 2D parameter space can cause a Berry phase of $\pm\pi$ in a wavefunction whose instantaneous eigenenergy has a diabolical point enclosed in this circle [19]. Since the position of the diabolical point in the $d_x - d_y$ plane is determined by (k_x, k_y) , the Berry phase acquired by the fermions with different momenta are different: It is $\pm\pi$ for the fermions whose diabolic point $(d_x = \mp t_0 k_y l_0 / \lambda, d_y = \pm t_0 k_x l_0 / \lambda)$ is enclosed in the track, while it is zero for the states with the diabolical point in the $d_x - d_y$ parameter space outside the track.

The above conclusion about the Berry phase is valid only in the adiabatic condition, i.e., the energy difference between two bands is always much larger than $\hbar\omega$ in the track. There exist fermion states for which the adiabatic condition can not be satisfied. In this case we have to investigate the geometric phase from solutions of time-dependent Hamiltonian. In a periodic time-dependent Hamiltonians the wavefunctions can be expressed in the Floquet form [20, 21]. This scheme has been used to solve the states in a laser field in calculation of the harmonics generation in graphene [22] and in nanotube [23]. In periodic vibrations of d_x and d_y the electron wavefunction can be written as

$$\psi^{\pm}(l, \mathbf{k}, t) = e^{-i \frac{\epsilon^{\pm}(l, \mathbf{k})}{\hbar} t} u^{\pm}(l, \mathbf{k}, t), \quad (9)$$

where l is an index of electron states for given \mathbf{k} , and $u^\pm(l, \mathbf{k}, t)$ is a periodic function of t with period $T = \frac{2\pi}{\omega}$. Performing Fourier transformation for $u^\pm(l, \mathbf{k}, t)$ with respect to t , one has

$$u^\pm(l, \mathbf{k}, t) = \sum_n \begin{pmatrix} A_n^\pm(l, \mathbf{k}) \\ B_n^\pm(l, \mathbf{k}) \end{pmatrix} e^{-in\omega t}, \quad (10)$$

where A_n^\pm and B_n^\pm are components on two sublattices. Substituting the Floquet wave function into the time-dependent Schrödinger equation $[H_\pm(t) - i\hbar\partial_t]\psi^\pm(l, \mathbf{k}, t) = 0$, we obtain a set of linear homogeneous equations for the components

$$\frac{3t_0l_0}{2}(\pm k_y + ik_x)B_n^\pm + \frac{3}{4}(e^{i\alpha_x}\eta_x \mp ie^{i\alpha_y}\eta_y)B_{n-1}^\pm + \frac{3}{4}(e^{-i\alpha_x}\eta_x \mp ie^{-i\alpha_y}\eta_y)B_{n+1}^\pm = (\epsilon^\pm + n\hbar\omega)A_n^\pm, \quad (11)$$

$$\frac{3t_0l_0}{2}(\pm k_y - ik_x)A_n^\pm + \frac{3}{4}(e^{i\alpha_x}\eta_x \pm ie^{i\alpha_y}\eta_y)A_{n-1}^\pm + \frac{3}{4}(e^{-i\alpha_x}\eta_x \pm ie^{-i\alpha_y}\eta_y)A_{n+1}^\pm = (\epsilon^\pm + n\hbar\omega)B_n^\pm. \quad (12)$$

From the requirement of nonzero solutions, for given \mathbf{k} one can solve the discrete quasienergies $\epsilon^\pm(l, \mathbf{k})$ and the corresponding Floquet states $\psi^\pm(l, \mathbf{k}, t)$. It is noteworthy that two Floquet states whose quasienergies differ by $n\hbar\omega$ with n being an integer are physically equivalent states [21]. So the quasienergies of physically different Floquet states can be reduced into region $-\frac{\hbar\omega}{2} \leq \epsilon^\pm \leq \frac{\hbar\omega}{2}$.

In a period the wavefunction $\psi^\pm(l, \mathbf{k}, t = T) = e^{i\phi^\pm(l, \mathbf{k})}\psi^\pm(l, \mathbf{k}, t = 0)$ acquires a phase $\phi^\pm(l, \mathbf{k})$. It consists of two parts: $\phi^\pm(l, \mathbf{k}) = \alpha^\pm(l, \mathbf{k}) + \beta^\pm(l, \mathbf{k})$, where $\alpha^\pm(l, \mathbf{k}) = -\frac{\bar{E}^\pm(l, \mathbf{k})T}{\hbar}$ is the dynamical phase with $\bar{E}^\pm(l, \mathbf{k}) = \frac{1}{T} \int_0^T dt \langle \psi^\pm(l, \mathbf{k}, t) | H_\pm(t) | \psi^\pm(l, \mathbf{k}, t) \rangle$, and $\beta^\pm(l, \mathbf{k}) = \phi^\pm(l, \mathbf{k}) - \alpha^\pm(l, \mathbf{k})$ is the geometrical phase [24]. Under the periodic vibrations the Floquet state $\psi^\pm(l, \mathbf{k}, t)$ is stationary one which returns to the initial state other than phase $\phi^\pm(l, \mathbf{k}) = -\frac{2\pi\epsilon^\pm(l, \mathbf{k})}{\hbar\omega}$ after a period of evolution. At the same time, the energy is no longer a good quantum number and the average energy of stationary state $\psi^\pm(l, \mathbf{k}, t)$ can be calculated as

$$\bar{E}^\pm(l, \mathbf{k}) = \epsilon^\pm(l, \mathbf{k}) + \hbar \sum_n n\omega (|A_n^\pm(l, \mathbf{k})|^2 + |B_n^\pm(l, \mathbf{k})|^2). \quad (13)$$

From this one obtains the geometric phase

$$\beta^\pm(l, \mathbf{k}) = 2\pi \sum_n n (|A_n^\pm(l, \mathbf{k})|^2 + |B_n^\pm(l, \mathbf{k})|^2). \quad (14)$$

The energy uncertainty caused by the vibration can be specified by the standard variance

$$\begin{aligned} \Delta^\pm(l, \mathbf{k}) &\equiv \langle E^2 \rangle - \langle E \rangle^2 \\ &= \hbar^2\omega^2 \left\{ \sum_n n^2 (|A_n^\pm(l, \mathbf{k})|^2 + |B_n^\pm(l, \mathbf{k})|^2) - \left[\sum_n n (|A_n^\pm(l, \mathbf{k})|^2 + |B_n^\pm(l, \mathbf{k})|^2) \right]^2 \right\}. \quad (15) \end{aligned}$$

From the superposition principle any time-dependent state can be expressed as a linear combination of the Floquet states. But this linear combination is usually not a stationary state, i.e., the state could not return to its initial one with only a phase difference after a period. For such states the geometric phase can not be defined. So in this paper we only consider the geometric phase for the Floquet states. Since for given valley and given momentum there are only two unknowns having the same phonon number n in Eqs. (11) and (12), the number of quasienergies within range of $[-\frac{\hbar\omega}{2}, \frac{\hbar\omega}{2}]$ is 2, corresponding to the lower and upper bands of the Dirac fermions with labels $l = 1$ and $l = 2$, respectively.

Now we begin to investigate the properties of stationary states in the periodic vibrations. We are interested in: (i) the geometric phases acquired by fermion states with various momenta in a period of vibrations; (ii) the deviation of the average energy from the Dirac

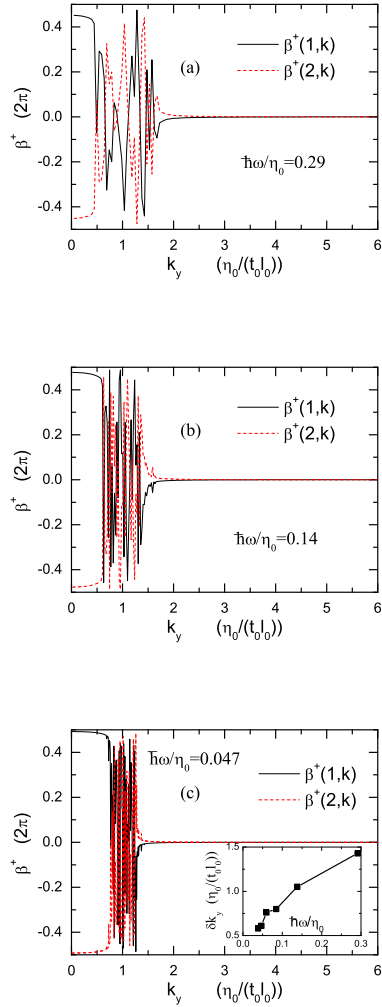


Fig. 2: (Color online) Geometric phase acquired in a period of vibrations by Dirac fermions in lower and upper bands of valley “+” as a function of the fermion momentum. The parameters for vibrations are: $\eta_x = \eta_y = \eta_0$, $\alpha_x = 0$, and $\alpha_y = -\frac{\pi}{2}$. $k_x = 0$ and units of k_y are set to be $\frac{\eta_0}{t_0 l_0}$ so that the border between the $\pm\pi$ Berry phase and the zero Berry phase is at $k_y = 1$. The inset of (c) shows the width of the chaotic region δk_y as a function of the frequency.

dispersion relation and the energy uncertainty caused by the vibration. From (i) we can shed some light on the phase variation of Dirac fermions. From (ii) we can see the essential effect of vibrations on the basic energy spectrum.

In Fig. 2 we plot the geometric phase acquired by fermion states in a period of vibrations versus the fermion momentum. There is a $\frac{\pi}{2}$ phase difference between the vibrations in the x and y directions and their amplitudes are the same, i.e., $\eta_x = \eta_y = \eta_0$. So this is a circular vibration of the relative coordinates of two sublattices as shown in Fig. 1. According to the Berry theorem, the adiabatic Berry phase is $\pm\pi$ if $|\mathbf{k}| < \frac{\eta_0}{t_0 l_0}$ and is zero if $|\mathbf{k}| > \frac{\eta_0}{t_0 l_0}$. We note that from the calculations beyond the adiabatic approximation the obtained geometric phase is still roughly equal to the Berry phase: for $|\mathbf{k}| \ll \frac{\eta_0}{t_0 l_0}$ it is nearly $\pm\pi$ and for $|\mathbf{k}| \gg \frac{\eta_0}{t_0 l_0}$ it is almost zero. However, now there appears a “chaotic” region

around the border $|\mathbf{k}| = \frac{\eta_0}{t_0 l_0}$ where the geometric phase randomly oscillates in changing the momentum. This is a direct consequence of the non-adiabaticity, as in this region the adiabatic condition, that the energy difference between two bands is much larger than $\hbar\omega$ in the evolution path, is not satisfied. As can be seen from the inset of Fig. 2(c), the width of this chaotic region is increased by increasing the frequency. The chaotic nature of the geometric phase reflects the phase uncertainty of the single-fermion states in this momentum region during vibrations. Such vibrations may exist in the graphene due to thermal excitations, or due to the zero-point fluctuations. Especially, the Berry phase effect may produce Born-Huang vibronic centrifugal term (see below) which may cause nonzero vibrations even at very low temperature. So such a fermion-lattice interaction can play roles of a dephasing mechanism for the single-fermion states. We also note that in the whole region, even including the chaotic region, the geometric phases acquired by fermions of the same momentum in two bands are opposite to each other. This phase compensation effect of two bands implies that this dephasing mechanism has no effect if the fermions in two bands are paired. The exchange of two bands leads to the sign reverse of the geometric phase. From the symmetry shown in Fig. 1 we can see that an equivalent operator which can also cause the sign reverse of the geometric phase is the reverse of the direction of the circular vibration from clockwise to counterclockwise or vice versa.

Another significant effect of vibrations is the change of fermion energies. As the single-particle energy is not a good quantum number, in Fig. 3 we plot the average energy of single-fermion states as a function of the momentum. From the comparison with the Dirac dispersion relation and with Fig. 2, the energy difference between two bands is enlarged near the Dirac point and for $|\mathbf{k}| \gg \frac{\eta_0}{t_0 l_0}$, where the geometric phase is near its adiabatic value, $\pm\pi$ or zero, while this energy difference shrinks in the chaotic region where the adiabatic approximation can not be used. Such opposite behaviors in these two regions imply that the failure of the adiabatic theory in the chaotic region has much more profound meaning than reflected from the values of geometric phase. Physically, in the chaotic region the oscillations of electrons between two bands are not able to follow the vibrations, this causes the loss of distinguishability of the two bands and the resultant states trend to take average energies in between, leading to a smaller energy spacing. On the contrary, in a quantum description the coupling of two states always enlarges their energy spacing. So one may expect that the chaotic region corresponds to a classical-like behavior and has a maximum uncertainty of single-fermion energies.

The total average energy of fermions V_e is then also changed and becomes dependent on the vibration amplitude η_0 . In the inset of Fig. 3(a) we plot the effective potential $V(\eta_0) = \frac{1}{2}g\eta_0^2 + V_e(\eta_0)$ where the first term is the ordinary elastic potential. The minimum is shifted from the center (Born-Huang vibronic centrifugal term), leading to nonzero vibrations even at very low temperature.

We calculate the standard variance of Eq. (15) and show the results in Fig. 4. As expected, the standard variance exhibits spikes in the chaotic region, and the energy uncertainty increases by increasing the amplitudes of vibrations. Except for the spikes in the chaotic region, the standard variance globally increases by increasing the momentum. Especially, the energy uncertainty becomes zero at the Dirac point for all the investigated vibration amplitudes. This originates from the fact that the energy uncertainty is due to the oscillation of the fermion states between two bands, but at the Dirac point the two bands coincide, leading to a zero amplitude of the oscillation. This structure, including the spikes and the globally increasing background with the momentum, may catch major features of linewidth distribution obtained from the angle-resolved photoemission spectroscopy in graphene [25]. Spikes also appear in the average energy of electrons in quasi-1D nanotube under periodic laser field [23], but in the present case the spikes occur in 2D momentum space originating from specific electron-phonon interaction in graphene and are closely related to the geometric phase.

The evolution path plays a crucial role on the distribution of adiabatic and chaotic

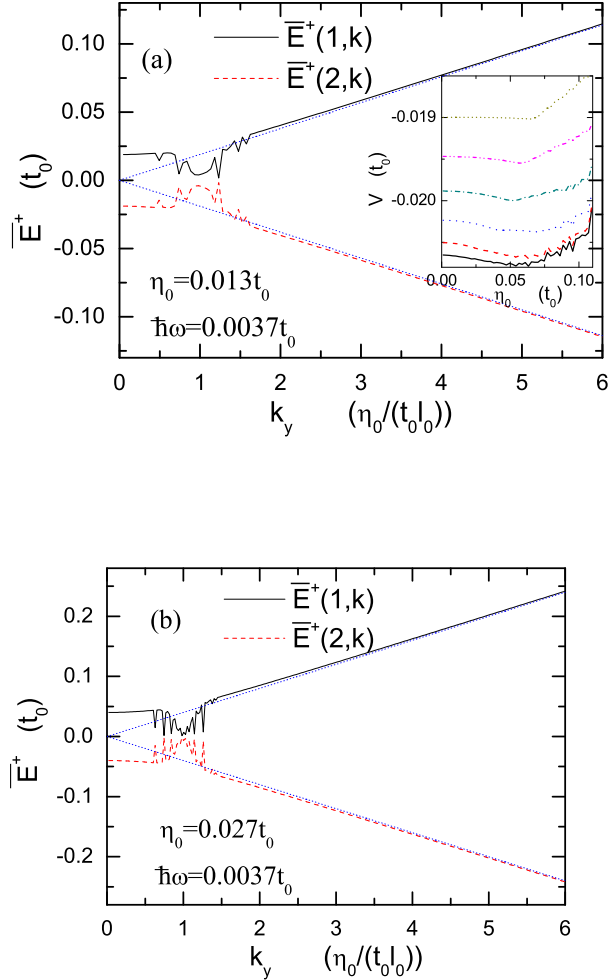


Fig. 3: (Color online) Average energy of fermions in lower and upper bands of valley “+” as a function of the fermion momentum. The parameters for vibrations are $\eta_x = \eta_y = \eta_0$, $\alpha_x = 0$, and $\alpha_y = -\frac{\pi}{2}$. $k_x = 0$. The blue dotted lines represent eigenenergies without vibrations. Inset in (a): The effective potential of vibrations as a function of rescaled displacement η_0 for different carrier densities. For curves from bottom to top the extra electron densities above the Dirac point are: 0, 0.00054, 0.00108, 0.00162, 0.00216, 0.0027 per atom. $\hbar\omega = 0.0037t_0$ and $g = 0.25/t_0$.

regions in the momentum space. To show this in Fig. 5 we plot the geometric phase as a function of k_x and k_y for an elliptic path. The chaotic region forms an orbicular area with a nearly fixed width along a loop defined by $k_x = \frac{\lambda d_y(t)}{t_0 t_0}$ and $k_y = -\frac{\lambda d_x(t)}{t_0 t_0}$. The width depends on ω as shown in the inset of Fig. 2(c). As a result, the adiabatic region with a $\pm\pi$ Berry phase is compressed by reducing the short axis of the ellipse, but the chaotic region with random geometric phases can exist even for a linear vibration.

In summary, we investigate the geometric phase and the change of dispersion relation of fermion states under relative vibrations of two sublattices in graphene. For a circular vibration there are two regions in the momentum space: in one region the geometric phase

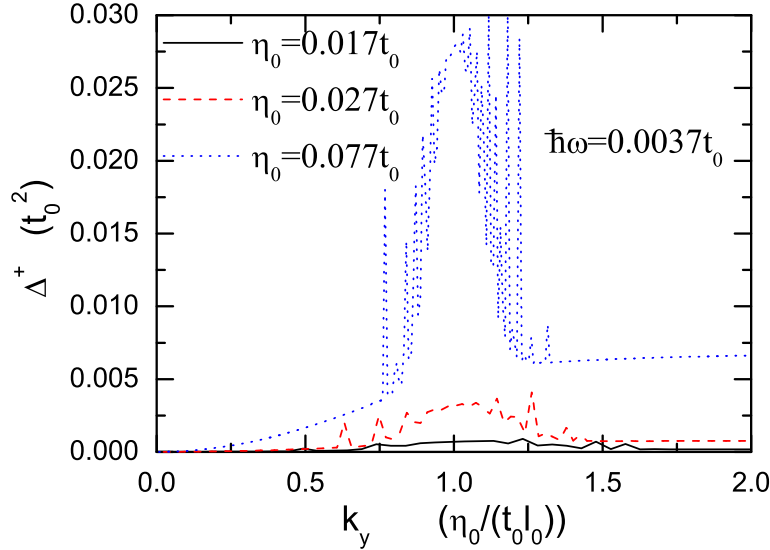


Fig. 4: (Color online) Standard variance of single-fermion energy of valley “+” as a function of the fermion momentum. The parameters for vibrations are $\eta_x = \eta_y = \eta_0$, $\alpha_x = 0$, and $\alpha_y = -\frac{\pi}{2}$. $k_x = 0$. The standard variance is the same for lower and upper bands.

acquired by the fermion states can be approximated by the adiabatic Berry phase and the average energy spacing between two bands is enlarged; in the other region the geometric phase exhibits random oscillations in changing the momentum, much different from the adiabatic value, and the average energy spacing shrinks. The energy uncertainty of fermions due to vibrations shows spikes in the chaotic region. For elliptic paths of vibrations the distribution of the adiabatic and chaotic regions crucially depends on the path shapes. The results suggest a possible dephasing mechanism which causes classical-like transport properties in graphene.

This work was supported by the State Key Programs for Basic Research of China (2005CB623605 and 2006CB921803), and by National Foundation of Natural Science in China Grant Nos. 10474033, [10704040](#), and 60676056.

REFERENCES

- [1] NOVOSELOV K. S. *et al.*, *Science*, **306** (2004) 666.
- [2] BERGER C. *et al.*, *J. Phys. Chem. B*, **108** (2004) 19912.
- [3] NOVOSELOV K. S. *et al.*, *Nature (London)*, **438** (2005) 197.
- [4] ZHANG Y., TAN Y.-W., STORMER H.L. and KIM P., *Nature (London)*, **438** (2005) 201.
- [5] BERGER C. *et al.*, *Science*, **312** (2006) 1191.
- [6] MOROZOV S.V. *et al.*, *Phys. Rev. Lett.*, **97** (2006) 016801.
- [7] PEREIRA V. M. *et al.*, *Phys. Rev. Lett.*, **96** (2006) 036801.
- [8] KHVESHCHENKO D.V., *Phys. Rev. Lett.*, **97** (2006) 036802.

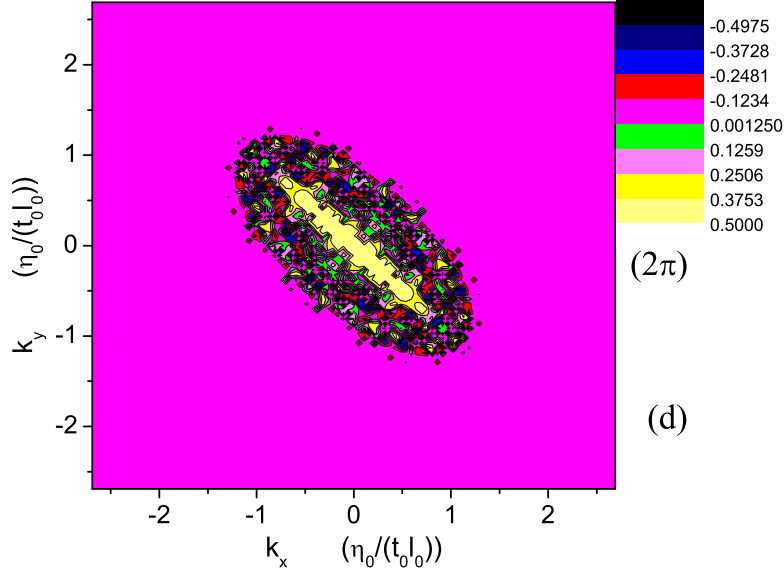


Fig. 5: (Color online) Contour plot of geometric phase acquired by fermions in valley “+” and in the upper band as a function of k_x and k_y . The parameters for vibrations are $\eta_x = \eta_y = \eta_0 = 0.078t_0$, $\hbar\omega = 0.0037t_0$, $\alpha_x = 0$, and $\alpha_y = 0.6$.

- [9] McCANN E., KECHEDZHI K., FAL’KO V.I., SUZUURA H., ANDO T. and ALTSHULER B.L., *Phys. Rev. Lett.*, **97** (2006) 146805.
- [10] MORPURGO A.F. and GUINEA F., *Phys. Rev. Lett.*, **97** (2006) 196804.
- [11] ALEINER I.L. and EFETOV K.B., *Phys. Rev. Lett.*, **97** (2006) 236801.
- [12] ALTLAND A., *Phys. Rev. Lett.*, **97** (2006) 236802.
- [13] ZIEGLER K., *Phys. Rev. Lett.*, **97** (2006) 268802.
- [14] NOMURA K. and MACDONALD A.H., *Phys. Rev. Lett.*, **98** (2007) 076602.
- [15] SHARAPOV S.G., GUSYNIN V.P. and BECK H., *Phys. Rev. B*, **69** (2004) 075104; LUKYANCHUK I.A. and KOPELEVICH Y., *Phys. Rev. Lett.*, **93** (2004) 166402.
- [16] LAZZERI M. and MAURI F., *Phys. Rev. Lett.*, **97** (2006) 266407; PISANA S. *et al.*, *arXiv, cond-mat* (2006) 0611714; ANDO T., *J. of Phys. Soc. of Japan*, **76** (2007) 024712.
- [17] SLONCZEWSKI J.C. and WEISS P.R., *Phys. Rev.*, **109** (1958) 272.
- [18] SUZUURA H. and ANDO T., *Phys. Rev. B*, **65** (2002) 235412; ISHIKAWA K. and ANDO T., *J. of Phys. Soc. of Japan*, **75** (2006) 084713.
- [19] BERRY M.V., *Proc. R. Soc. London A*, **392** (1984) 45.
- [20] FLOQUET A.M.G., *Ann. Ecole Norm. Sup.*, **12** (1883) 47.
- [21] SAMBE H., *Phys. Rev. A*, **7** (1973) 2203.
- [22] GUPTA A.K., ALON O.E. and MOISEYEV N., *Phys. Rev. B*, **68** (2003) 205101.
- [23] HSU H. and REICHL L.E., *Phys. Rev. B*, **74** (2006) 115406.
- [24] AHARONOV Y. and ANANDAN J., *Phys. Rev. Lett.*, **58** (1987) 1593.
- [25] BOSTWICK A., OHTA T., SEYLLER T., HORN K. and ROTENBERG E., *Nature Physics*, **3** (2007) 36.